Micromachined Array of Electrostatic Energy Analyzers for Charged Particles

R.E. Staider, S. Boumsellek, T.R. VanZandt, T.W. Kenny, M.H. Hecht, F.E. Grunthaner

Jet Propulsion Laboratory, 4800 Oak Grove Drive, Pasadena, CA 91109, USA

Abstract

The design, fabrication techniques and first test results of a new type of micromachined energy analyzer for charged particles are presented. The novel design is based cm a Bessel Box straight-line geometry with focusing in one dimension. The problem of small acceptance area due to the drastically reduced overall dimensions is accounted for by the use of a parallel array of small analyzers simultaneously. We describe the fabrication of a proof-of-concept micromachined Bessel Box array by means of an isotropic wet-etching of <110> silicon, and we present ray-tracing simulations for a simple geometry. Finally we show some test results of Auger electrons and discuss possible applications of generic small charged particle analyzers.

Abstract # : 1028
Program # : NS-MoM8
Put on JVST manuscript

40th American Vacuum Society Symposium
November 15-19, 1993
Orlando, Florida

I. Introduction

Electrostatic lenses for charged particles optics are usually bulky but of fairly simple shape and they have to be machined with stringent tolerances. Fundamental limitations such as spherical aberrations result in lens diameters much larger than the useful beam width, e.g. in.* electron microscopy. There are however, a number of applications where the size of electrostatic lenses could be reduced significantly without loss of performance. One area of special interest has been identified with the mass and energy detection of ions and electrons. In the general context of building smaller spacecraft for the robotic exploration of the solar system and outer space, the reduction of mass, volume and power of scientific payloads is badly needed. However, the signal level of telescopes and detectors is usually proportional to the acceptance area and hence one would like to have this instrument dimension large in order to collect as much signal as possible. Consider a charged particle detector with given volume, mass and aperture area (Figure 1). By simply reducing the linear dimensions of the device by a factor of n the volume and the mass scale down by r?. However, the area of the aperture scales down as n^2 and thus the smaller device collects n times more signal per unit mass (and unit volume). If we therefore recover the original signal level by using a 2-dimensional array with n^2 small devices, this array has the same acceptance area as the original device but its mass and volume are smaller by a factor of n each. Whenever the reduction of the aperture size has no other severe drawbacks (e.g. in a diffraction limited telescope) the use of an array of small instruments replacing a large one offers an interesting solution for building smaller and lighter instruments without loss of signal. The currently developed techniques of micromachining three-dimensional structures with very high precision offer a method to reduce the size of electrostatic analyzers significantly.

11. The conventional Bessel Box

A diagram of a Bessel Box acting as an energy (i.e. energy/charge for multiple charged ions) bandpass filter for charged particles is shown in Figure 2. Bessel Boxes as introduced by

Allen et. al. [1] are very simple electrostatic analyzers with a straight-line geometry. The basic concept is a can with two holes, one on top and one on the bottom representing the entrance and the exit apertures, and a beam stop in the center of the device [2]. Other designs use additional entrance and exit lenses as published by Lindau et. al. [3]. Low-energy cutoff is achieved by applying a DC voltage AV on' the end caps against the central cylindrical part of the box. The charged particles entering the box are thus forced to pass a potential barrier before reaching the exit aperture. A central beam stop prevents high-energy, on-axis particles from passing the filter and results in a high-energy cutoff, because the high-energy off-axis particles are not deflected by a sufficient amount to be focused into the exit aperture. The bandpass E_p of the energy filter will be centered just above the height VP of the central potential barrier, whereas the energy resolution is a function of the geometrical dimensions and scales linearly with the potential difference AV between the two end caps and the middle part. Typical dimensions of a conventional Bessel Box are about 10 cm in length and 5 cm in diameter. This is large compared to recently published reports of micromachined electron optical systems [4,5,6]. -

III. 'I'he micromachined Bessel Box

We have designed and built a micromachined Bessel Box with a length of 2.6 mm and a width of 0.8 mm. The first version of our design has a twofold rather than a cylindrical symmetry. The reason for the restriction to the l-dimensional focusing geometry was the compatibility with the crystallographic planes in the silicon crystal, which we chose for anisotropic etching [7]. Given the twofold symmetry of the $<110>$ crystal face, the device acts as an energy filter in one direction (x), whereas no focusing occurs in the perpendicular direction (y). Our first proof-of-concept prototype is an array of four micro Bessel Boxes with this simple linear geometry (Figure 3). The lateral distance between adjacent entrance slits is 1.6 mm. The micromachining of a Bessel Box with the more complicated cylindrical symmetry is possible by means of other techniques such as laser machining or LIGA.

The cross-section of the micromachined Bessel Box has a simple, array-compatible geometry as shown in Figure 4. Astackof seven <110> silicon wafers with thicknesses of either 0.2 mm or 0.8 mm is aligned within a few micrometers and bonded together. Each wafer carries a micromachined, freestanding grid with openings on the 100 micrometer scale. " These grids are fabricated by means of high aspect-ratio (i.e. deep but narrow structures) bulk etching of the silicon wafers with KOH using a thermally grown SiO_2 as an etching mask. In order to get a homogeneous surface function for the electrode areas, we use thin layers of titanium, platinum and gold deposited on the SiO_2 by e-beam evaporation. The exact distance between the electrodes is maintained by silicon spacers, covered with thermally grown SiO_2 of 1 micrometer thickness. The completed wafer stack has no open areas (all straight lines intersect at least one wafer), but by applying the appropriate electrostatic potential AV between the two cap wafers (B 1) and the middle part (132) the resulting electric field creates an array of electrostatic microlenses with a focal length depending on the kinetic energy of the particles.

We have calculated the performance of the micro Bessel Box by ray-tracing with the SIMION software [8]. -The calculations were carried out for an electrostatic potential barrier in the central drift part (B2) of the Bessel Box of V_p = -100 volts, and the entrance and exit planes (B1) were held at a potential $V_p - \Delta V$ = -90 volts. However, all the given voltages and kinetic energies can be scaled linearly. In Figure 5a-5c cross sections of a single microlens are given together with some ray-tracing results for electrons with different initial kinetic energies E_k. Low energy particles cannot pass the potential barrier V_p and are reflected whereas the deflection angle for high energy particles is not sufficient to bend them around the axial beam stop into the exit pupil. Particles with kinetic energy slightly above 100 eV can exit and will be selected by the analyzer. The selected energy E_k scales with the central potential barrier V_p. We computed ray-tracing for all different combinations of acceptance angle and entrance position for nine different kinetic energies ranging from 100.0 eV to 102..5 eV. An example of the calculated acceptance area in phase space is presented in Figure 6 for a kinetic energy of 101.5 eV. The resulting energy bandwidth ΔE (Figure 7) is about 1.2 eV full width at half

maximum (FWHM), or about 1/100 of the barrier height V_p for an applied voltage difference AV of VP/lO. The energy resolution scales linearly with the barrier height V_p and the voltage difference AV. The breakdown voltage for AV is high (in the kV range for a 1 micrometer thick layer of thermal SiO_2) and is therefore not of concern for high energy resolution.

Iv. Experimental Tests

We have performed experimental tests with a "shielded" version of the micro Bessel Box. The shielding consisted of placing two grounded grids (0.3 mtn mesh size) at a 1 mm distance from the two end caps (B 1) of the analyzer. We used ray-tracing calculations for studying the focusing effects on the electron trajectories. The shield distance was calculated for a maximum voltage of 500 volts applied to (B1), so that no penetrating fields will distort the motion of the electrons entering the Bessel Box and thus the resolution of the analyzer. The wire diameter of the grids is small (25 micrometers) compared to the width of the slits (100 micrometers) of the anal yzer. The grids constitute two arrays of grounded apertures for the array of micro lenses.

Experimental tests have been carried out using a set-up (Figure 8) consisting of an electron gun, a sample holder, the shielded micro Bessel Box and a secondary electron detector. The entire system was operated at a pressure of $6x10^{-8}$ Torr obtained with a 20 1/s ion pump. The electron optical anal ysis of the electron gun has been carried out for electron imaging at a moderate spatial resolution (20 microns). An aluminum-made holder has been designed to accommodate 1 cm^2 samples at a 450 angle with respect to the electron beam. Also assembled on the same holder are the energy filter and the secondary electron detector. The later is a Faraday cup provided with a grid biased slightly negative to prevent the escape of secondary electrons. The current of collected electrons is then amplified and read on an electrometer.

Initially, the incident electron beam has been focused to roughly 1 mm spot size using a phosphor screen at the sample location. The electron current is estimated to be 100 nA [9]. Cu and graphite were used to demonstrate the operation and also to establish accurate calibration

of the analyzer. Figure 9 shows electron spectra of copper and graphite, recorded in the kinetic energy of interest, in the integral form (left-hand side) and in the more familiar first derivative form (right-hand side). In the integral form, the low energy part of the secondary electron distribution can be seen as a large, very broad peak at a few electron volts and extending many tens of volts up the energy scale. On this continuous distribution are superimposed several Auger structures (C - KLL with graphite and Cu - MVV with copper) which are accentuated in the derivative form. The spectra were obtained at a primary beam energy of 1450 eV. The energy scale was calibrated by recording the analyzer voltage (B2) required to detect the elastic peak at several incident energies. Thus the carbon - KLL and the copper - MVV peaks were measured at 273.9 eV and 59.9 eV respectively, in fairly good agreement with the standard Auger spectra [10].

V. Conclusion

We have fabricated and tested a proof-of-concept device with four micrornachined Bessel Boxes. A geometry with focusing in one direction was micromachined in <110> silicon by means of anisotropic bulk etching with KOH. Preliminary test results measured with Auger electrons from two samples were shown. They agree well with the expectations from the computer simulations. Further characterizations (e.g. acceptance solid angle, resolution, transmission) are to be investigated to fully evaluate the analyzer. Also work is currently in progress to fabricate a 2-dimensional version of the array of micro Bessel Boxes using a minimum number of electrodes. Small electrostatic analyzers have many potential applications in space science (e.g. mass spectrometers) or as hand-held devices for chemical analysis.

VI. Acknowledgments

Valuable discussions with A. Chutjian and R. Goldstein and technical support from J.A. Podosek and S.J. Manion are gratefully acknowledged. One of the authors (R.E. Staider) acknowledges financial support by the Swiss National Science Foundation and by the National Research Council.

VII. References

[1] J.D. Allen Jr., J.P. Wolfe, G.K. Schweitzer, Int. J. Mass Spectrom. Ion Phys., 8, 81 (1972)

[2] J.H. Craig Jr. and W.G. Durrer, J. Vat. Sci. Technol. A7, 3337 (1989)

[3] I. Lindau, J.C. Helmer and J. Uebbing, Rev. of Sci. Instr. 44, 265 (1973)

[4] T.H.P. Chang , D.P. Kern and M.A. McCord, J. Vat. Sci. Technol. B8, 1855 (1989)

[5] T.H.P. Chang, D.P. Kern, and L.P. Muray, J. Vat. Sci. Technol. B8, 1698 (1990)

[6) L.P. Muray, U. Staufer, E. Bassous, D.P. Kern, T.H.P. Chang, J. Vat. Sci. Technol. B9, 2995 (1991)

[7] K.E. Petersen, Proceedings of the IEEE Vol. 70(S), 420 (1982)

[8] SIMION 4.0 software by D.A. Dahl, J.E. Delmore, Idaho National Engineering Laboratory, Idaho Falls, ID 83415, USA

[9] T. R. VanZandt, S. J. Manion, private communication

[10]L. E. Davies, N. C. MacDonald, P.W. Palmberg, G.E. Riach and R. Ii. Weber, Handbook of Auger -Electron Spectroscopy, Physical Electronics Division, Perkin Elmer Corporation, USA (1978)

VIII. Figure Captions

Figure 1.

The basic idea of recovering acceptance area at reduced mass and volume by applying 'an array of micromachined devices.

Figure 2.

Diagram of a conventional Bessel Box with cylindrical symmetry, operating as an energy-bandpass filter. The selected energy E_p is slightly higher than VP and the energy resolution ΔE scales linearly with AV.

Figure 3.

An array of four Bessel Boxes micromachined in <110> silicon. The distance between two entrance slits is 1.6 mm, the thickness of the device is 2.6 mm. All electrodes are covered with a thin Gold layer.

Figure 4.

Cross section trough the prototype array of four Bessel Boxes. The electrodes and spacers are made by a stack of seven anisotropically etched <110> silicon wafers. Wafers # 2 and # 6 are insulating spacers, wafers # 3, 4 and 5 are electrically connected.

Figure 5a-5c.

Ray tracing results calculated with the SIMION software for acceptance angle of +- 14 deg and kinetic energies E_k of 100.1 eV, 101.4 eV and 102.7 eV, respectively.

Figure 6.

Acceptance area in the x - ϕ_x phase-space for electrons with 101.5 eV. A similar acceptance area is found at negative acceptance angles. The width of the entrance slit in the x-direction is 100 micrometer.

Figure 7.

Calculated energy resolution. Ek is the component of the kinetic energy in the x-z plane of the Bessel Box.

Figure 8.

Schematic diagram of the experimental setup, showing the electron gun, the sample, the analyzer and the secondary electron detector,

Figure 9.

Energy spectra of electrons ejected from graphite (top) and copper (bottom) surfaces shown in the integral form (left-hand side) and in the first derivative form (right-hand side).

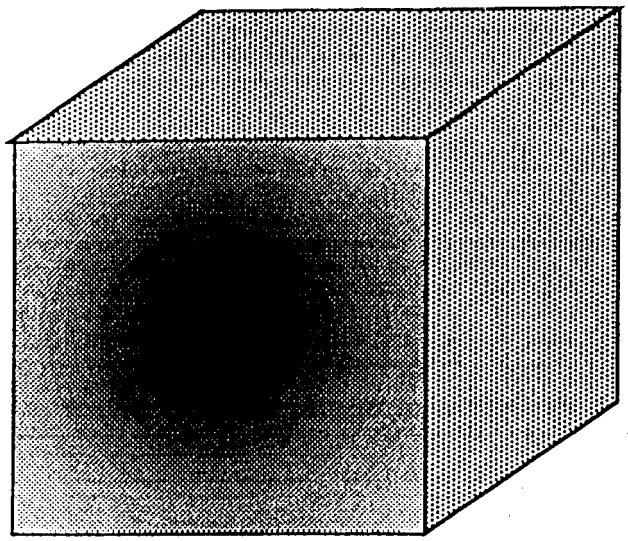

current device:

- volume =: 1
- mass =: 1
- aperture =: 1
- signal/mass = 1

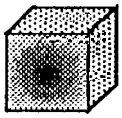

(l/n) -size device:

- volume = $(1/n^3)$
- mass = $(1/n^3)$
- aperture = $(1/n^2)$
- » signa I/mass = n

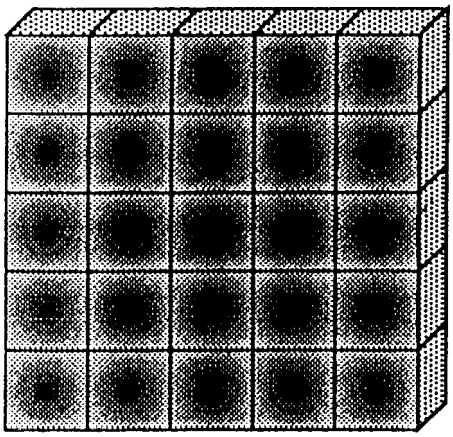

(1/n) device-array:

- volume = 1 / n
- mass = I/n
- » aperture = 1
- » signal/mass = n

Stalder et al. / Abstract # 1028 Figure 1

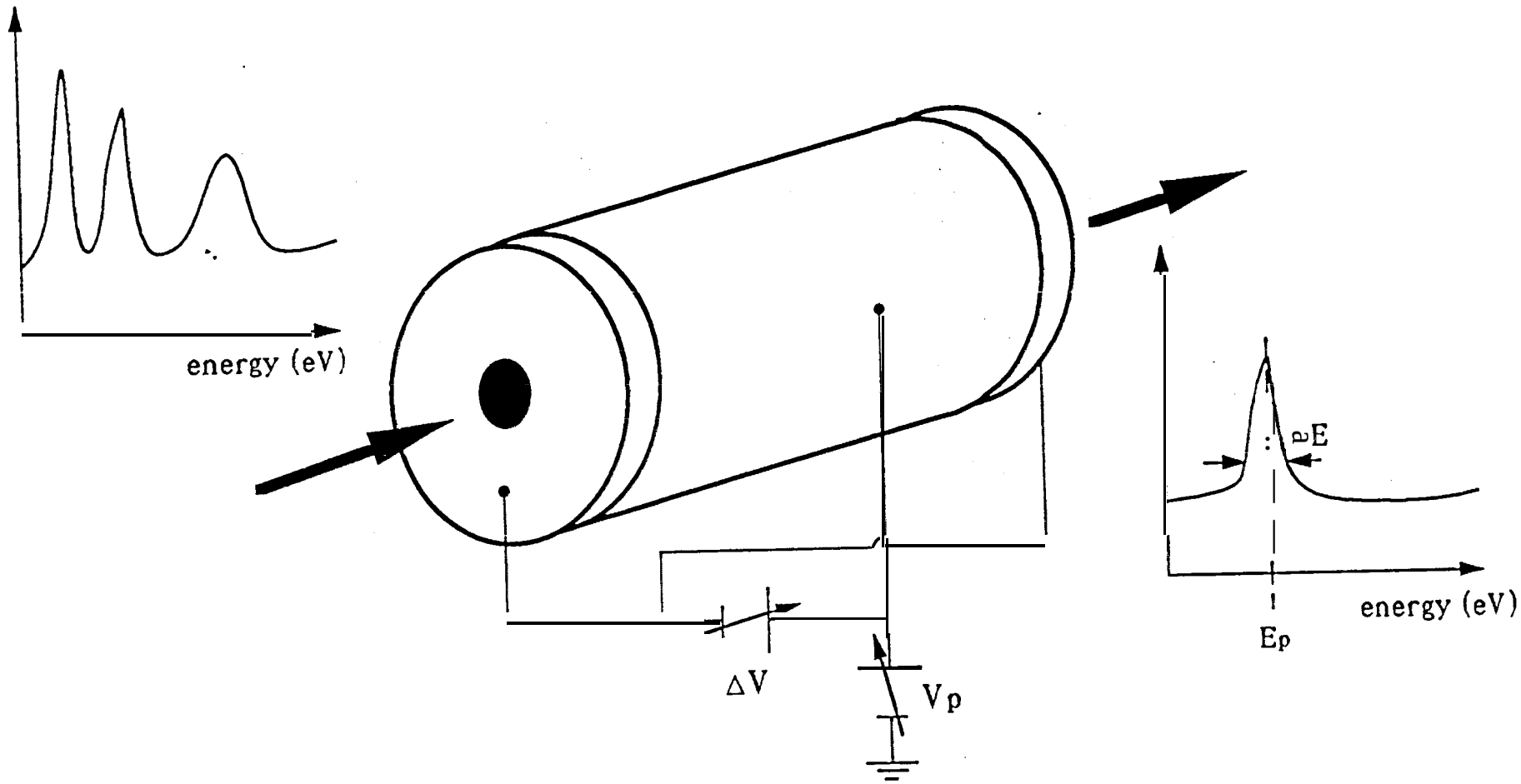
energy (eV)
ΔV
Vp
ΔE
Ep
energy (eV)

Schaller et al. / Abstract # 1028 Figure 3

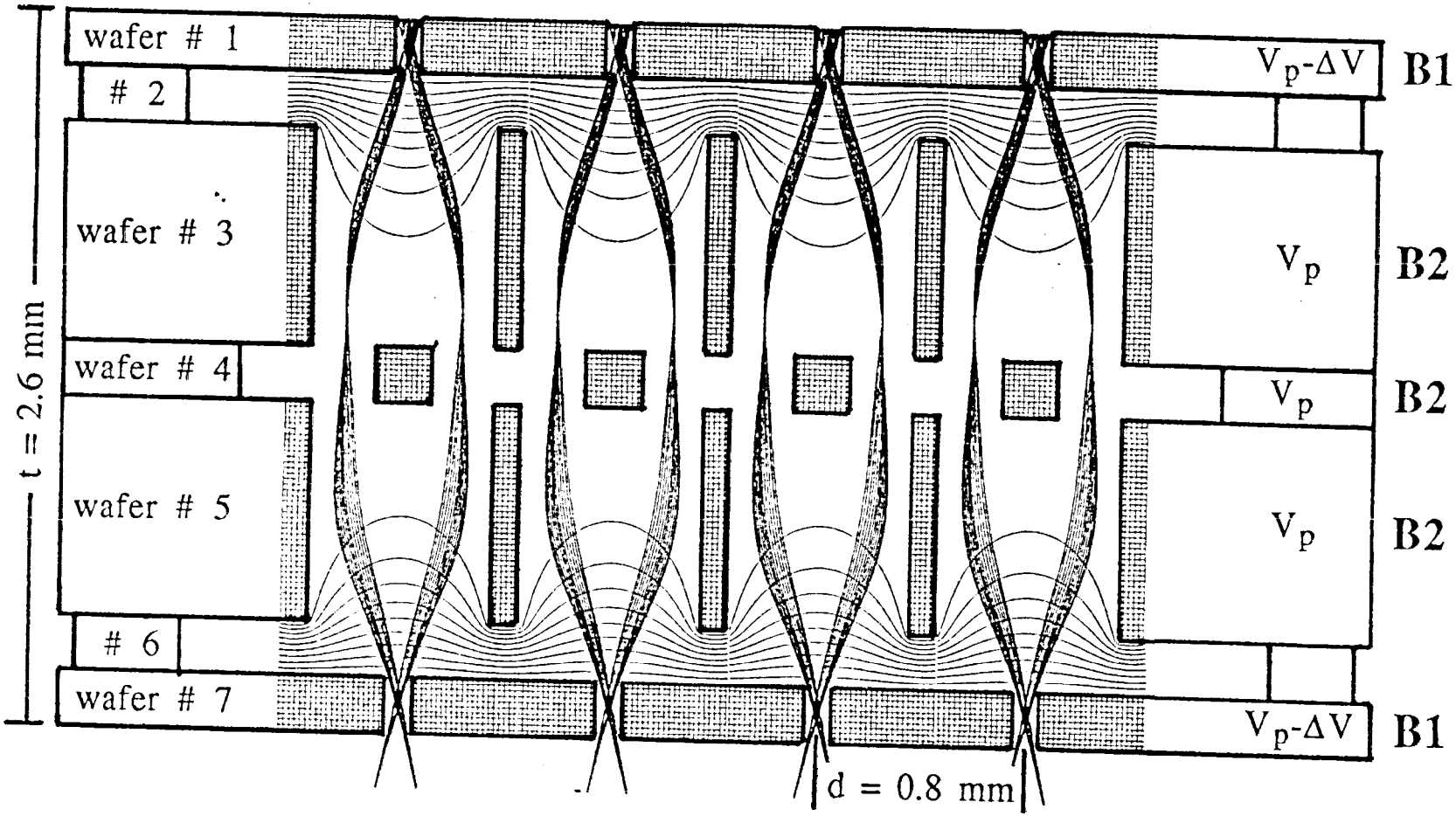
wafer # 1
2
wafer # 3
wafer # 4
wafer # 5
6
wafer # 7
t = 2.6 mm
V_p-ΔV
B1
V_p
B2
V_p
B2
V_p
B2
V_p-ΔV
B1
d = 0.8 mm

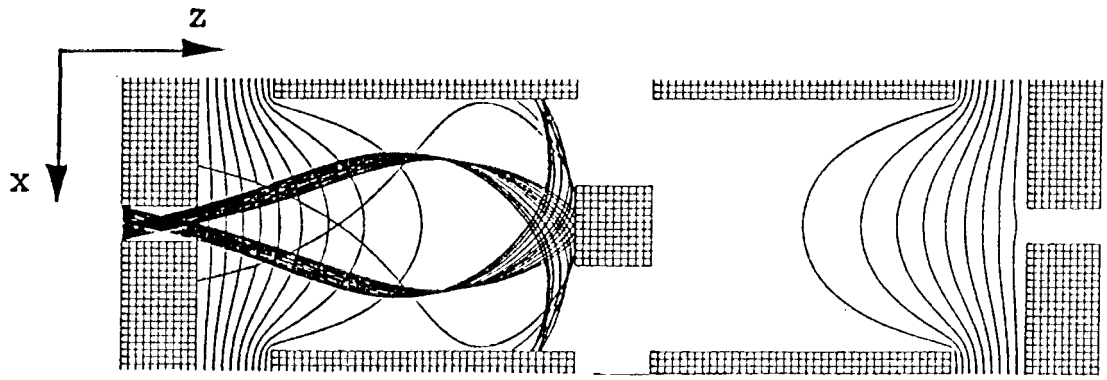

a 100.1 eV

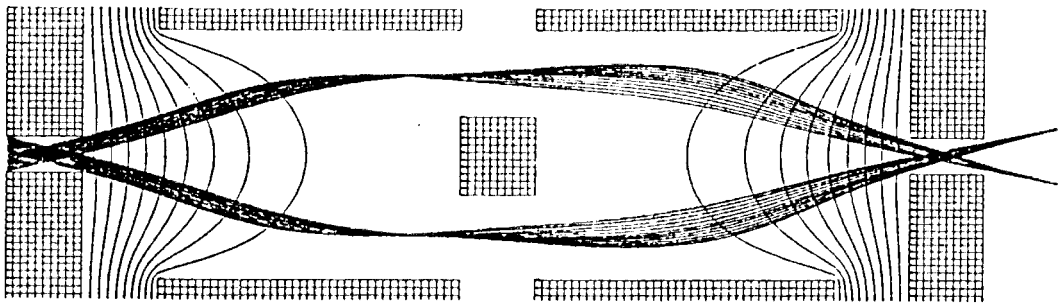

b 101.4 eV

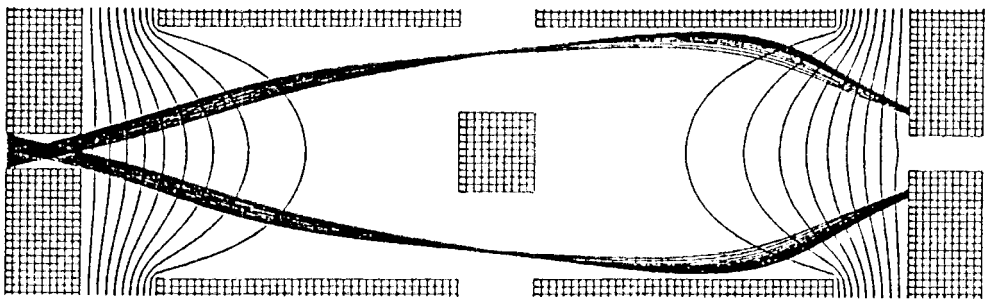

c 102.7 eV

Stalder et al. / Abstract # 1028 Figure 5

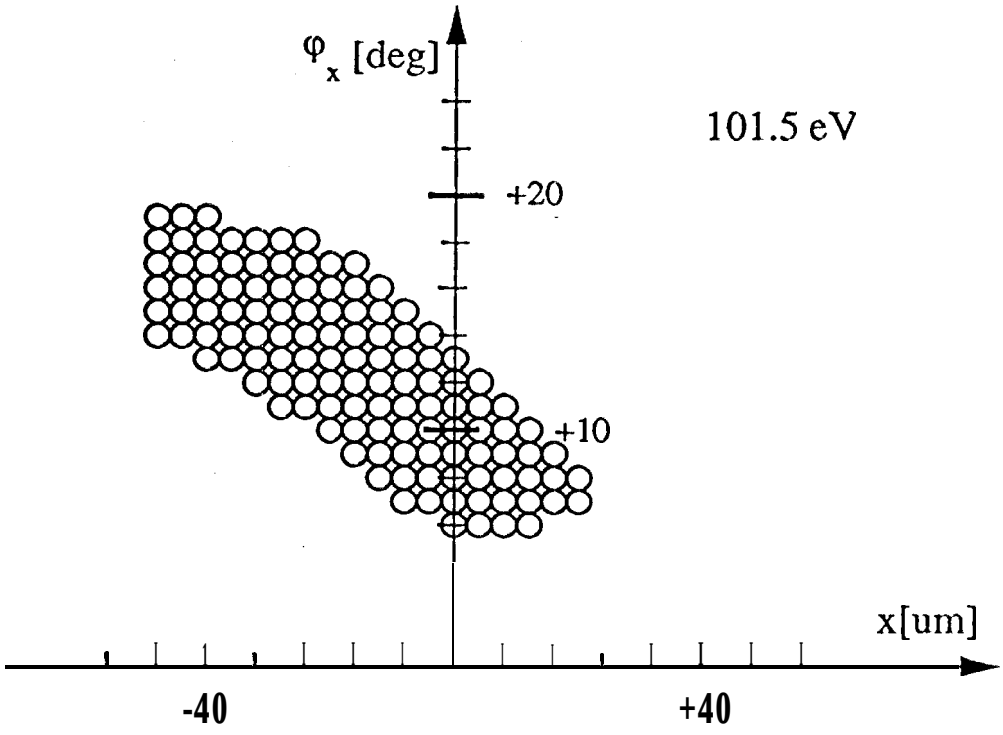

Stables et al. / Abstract # 1028 Figure 6

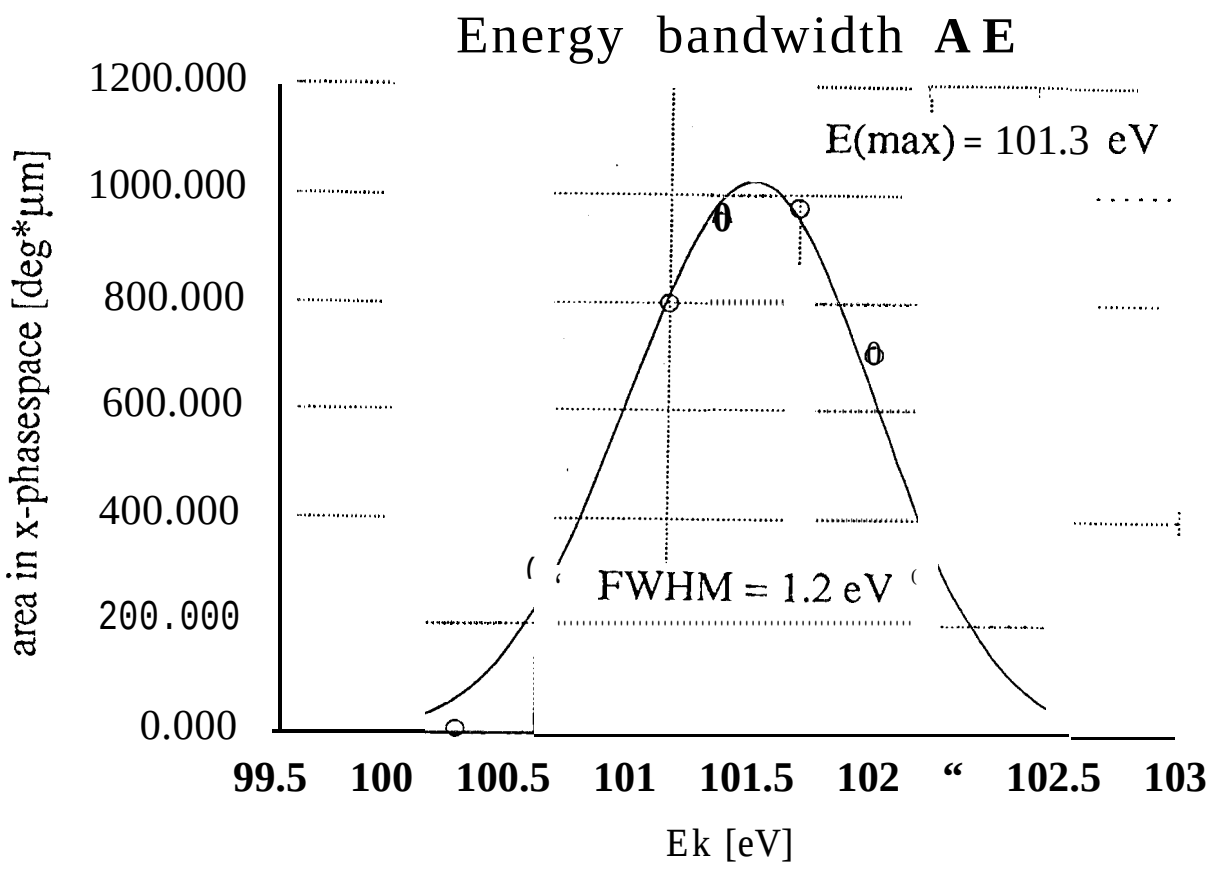

Stabler et al. / Abstract #1028 Figure 7

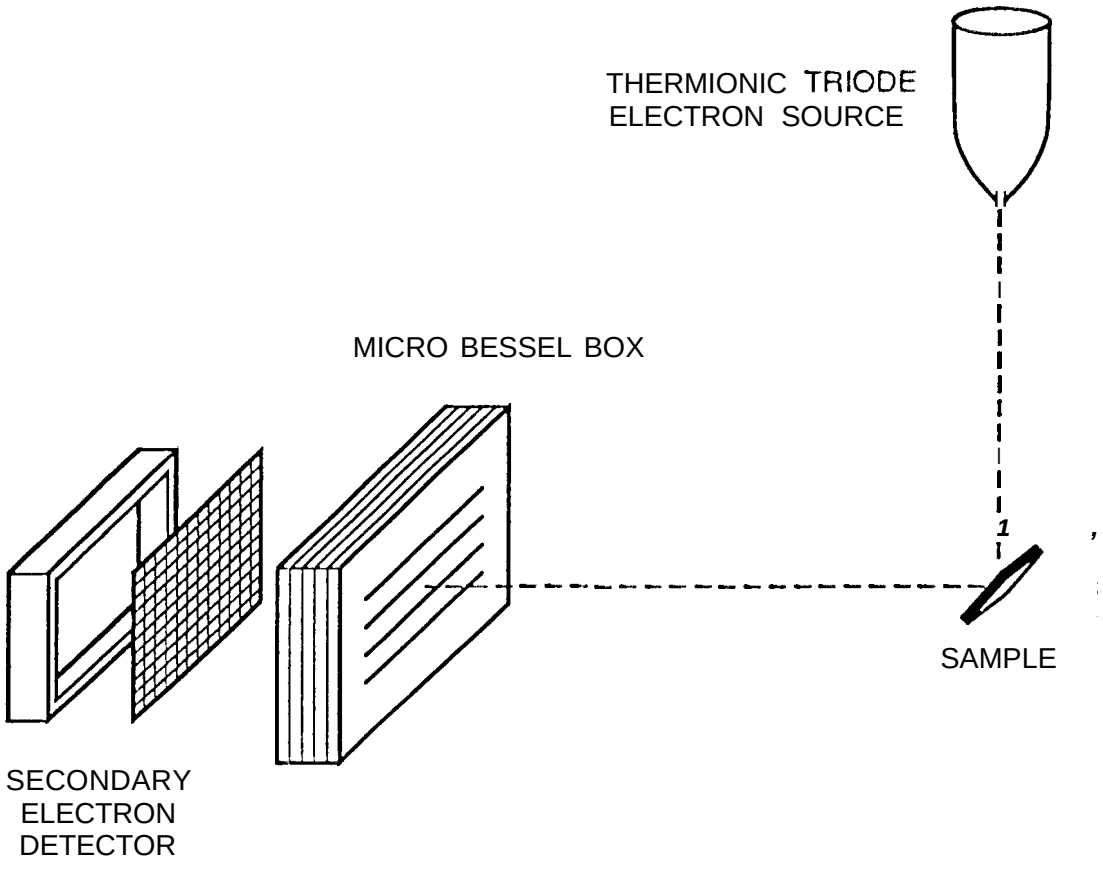

Stalder et al. / Abstract # 1028 Figure 8

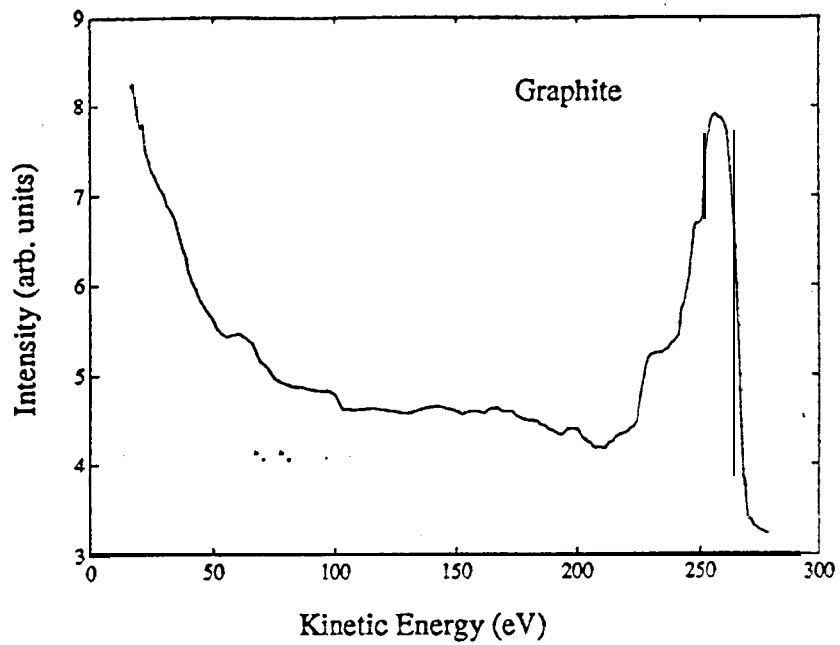
Graphite
Intensity (arb. units)
Kinetic Energy (eV)

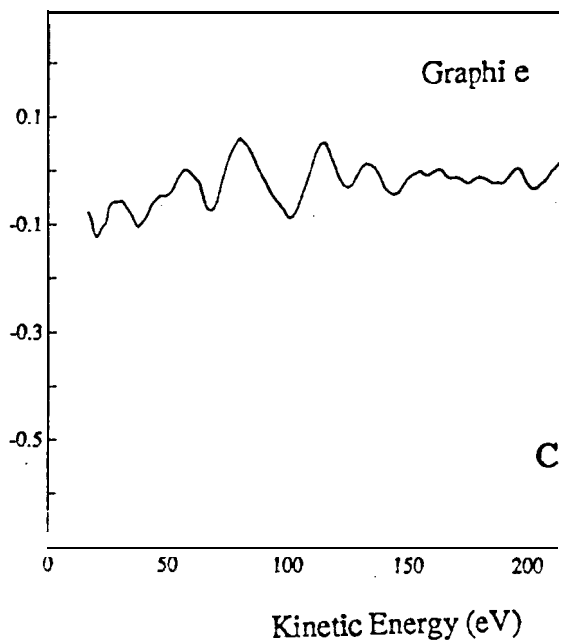
Graphi e
C
Kinetic Energy (eV)

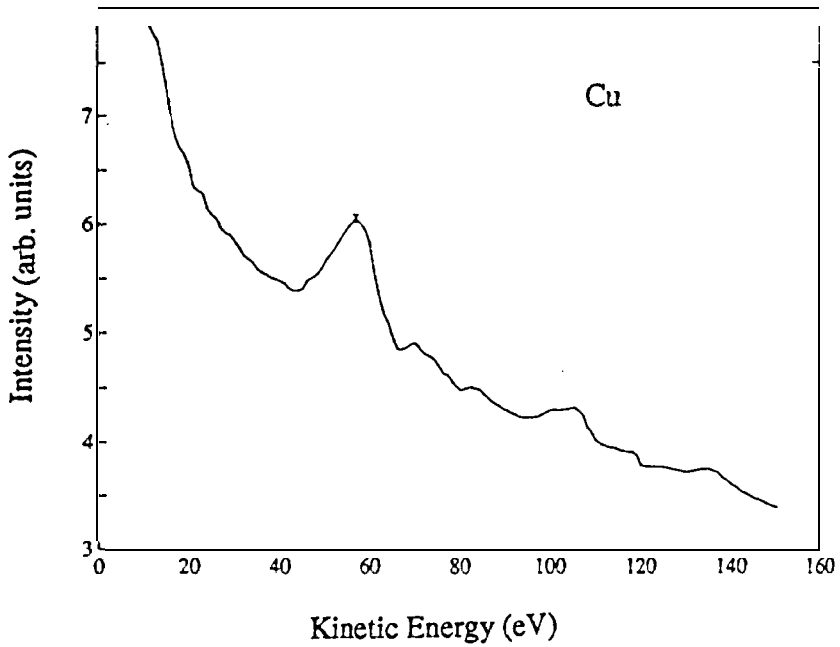
Cu
Intensity (arb. units)
Kinetic Energy (eV)

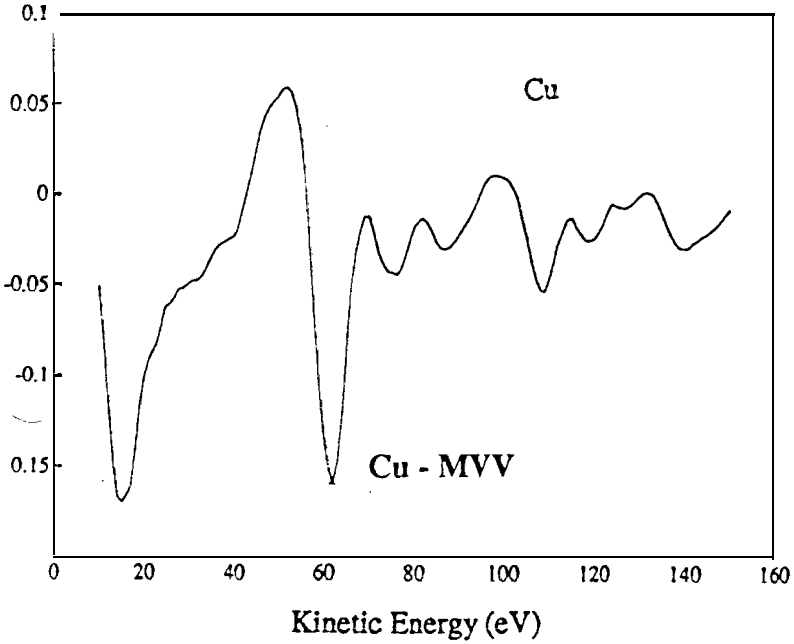
Cu
Cu - MVV
Kinetic Energy (eV)